Available online at www.sciencedirect.com
ScienceDirect
Ceramics International 38 (2012) 169–175
CERAMICS INTERNATIONAL
www.elsevier.com/locate/ceramint

In vitro bioactivity evaluation of magnesium-substituted fluorapatite nanopowders

M. Kheradmandfard [a,*], M.H. Fathi [a], M. Ahangarian [b], E. Mohammadi Zahrani [c]

[a] Biomaterials Research Group, Department of Materials Engineering, Isfahan University of Technology, Isfahan 8415683111, Iran
[b] Deptartment of Physics, Isfahan University of Technology, Isfahan 8415683111, Iran
[c] Department of Materials Engineering, University of British Columbia, Vancouver, B.C., V6T1Z4, Canada

Received 4 October 2010; received in revised form 12 May 2011; accepted 30 May 2011
Available online 1st July 2011

Abstract

Properties of apatites, such as bioactivity, biocompatibility, solubility, and adsorption properties can be tailored over a wide range by modifying the composition via ionic substitutions. The aim of this work was preparation, characterization and in vitro bioactivity evaluation of Mg-doped fluorapatite (Mg–FA) nanopowders. Mg–FA nanopowders with different Mg contents were prepared via sol–gel method. In vitro bioactivity evaluation of powders was performed by soaking the powders in simulated body fluid (SBF). Results indicated that Mg ions entered into the fluorapatite lattice and occupied Ca^{2+} sites, and the obtained powders had crystallite size about 30–100 nm. With increasing the Mg-substitution, the solubility of powders and the adsorption of Ca^{2+} ions onto the powders surfaces increased simultaneously. It was concluded that Mg-substitution improves the bioactivity of FA.

Keywords: A. Sol–gel processes; Nanopowder; Magnesium-substituted fluorapatite; Bioactivity; Simulated body fluid (SBF)

1. Introduction

Calcium phosphate bioceramics including apatites are in use, or being developed for implants in orthopedic and dental applications [1–3]. Fluorapatite ($Ca_{10}(PO_4)_6F_2$, FA) materials have been investigated as alternative biomedical materials [4–6]. Biological apatites contain many substitutions (i.e. Zn^{2+}, Mg^{2+}, F^{-}, CO^{-3}). These substitutions induce complex structures at the unit-cell level and play a role in influencing the dissolution rate of apatites, which may favour osteointegration [7–9]. Properties of apatites, such as bioactivity, biocompatibility, and solubility can be tailored over a wide range by modifying the composition via ionic substitutions. Magnesium (Mg) is one of the most important cationic substitutions for calcium in biological apatites. Dentin, enamel and bone contain 1.23, 0.44, and 0.72 wt% of Mg, respectively [10]. The presence of Mg makes the fluoridated hydroxyapatite (FHA) coatings more bioactive in promoting bone formation [11]. Liang et al. [12] found that Mg implantation improves the bioactivity of zirconia and titanium. Mg is strongly associated with mineralization of calcified tissues and directly stimulates osteoblast proliferation with an effect comparable to that of insulin [10,13].

In regard to the above points, Mg^{2+} substituted FA bioceramics are expected to have better biocompatibility and biological properties than pure FA. The essential requirement for artificial biomaterials to exhibit a bone bonding to living bone is the formation of a bone-like apatite (carbonate-containing hydroxyapatite) layer on its surface within a physiological environment [14,15]. Investigating the biological behavior of biomaterials in simulated body fluid (SBF), which has almost the same ion concentrations as those of human blood plasma, is considered as the most efficient and economical way to predict their bioactivity in body environment [16].

In the present work, Mg–FA nanopowders with different Mg contents were fabricated by sol–gel method. The fabricated nanopowders were soaked in SBF for evaluating their bioactivity via analyzing the formation of apatite on the surface of the powders.

* Corresponding author. Tel.: +98 311 3915708; fax: +98 311 3912752.
E-mail address: mkh_fard@yahoo.com (M. Kheradmandfard).

0272-8842/$36.00
doi:10.1016/j.ceramint.2011.05.157

2. Materials and methods

2.1. Preparation of Mg-substituted fluorapatite nanopowders

Mg-substituted fluorapatite nanopowders were prepared by sol–gel method. Calcium nitrate tetrahydrate ($Ca(NO_3)_2{\cdot}4H_2O$; Merck), magnesium nitrate hexahydrate ($Mg(NO_3)_2{\cdot}6H_2O$; Merck), phosphorus pentoxide (P_2O_5; Merck) and hexafluorophosphoric acid (HPF6; Floka) were selected to prepare Ca-precursor, Mg-precursor, P-precursor and F-precursor, respectively. A designated amount of phosphoric pentoxide (P_2O_5, Merck) was dissolved in absolute ethanol. Also, a designated amount of Mg-precursor and Ca-precursor was mixed to form the Ca–Mg mixture and then dissolved in absolute ethanol. This mixture was added drop-wise into the P-precursor to obtain a solution with (Ca, Mg)/P ratio of 1.67. Then, HPF_6 was added to the solution [11]. The designated degree of substitution of Ca^{2+} by Mg^{2+} in the mixture was determined by the x value in the general formula of FA ($Ca_{10-x}Mg_x(PO_4)_6F_2$), where $x = 0$, 0.25, 0.5, 0.75 and 0.1 [7]. The subsequent powders were labeled as FA0M, FA2.5M, FA5M, FA7.5M and FA10M, respectively. The mixture was continuously stirred for about 24 h at ambient temperature to form a gel. As-formed gel was aged for 24 h, and then it was dried in an oven at 100 °C in air for 24 h. The dried gel was sintered at 600 °C for 1 h in a muffle furnace.

2.2. Characterization

Phase structure analyses were carried out by X-ray diffraction (XRD) analysis using a Philips X'Pert-MPD diffractometer with Cu Kα radiation ($\lambda = 0.15418$ nm) over the 2θ range of 20–60°. The obtained experimental patterns were compared to the standards compiled by the Joint Committee on Powder Diffraction and Standards (JCDPS) which involved card # 15-0876 for FA. The crystallite size of prepared powders was determined using XRD patterns and Williamson–Hall approach [17].

Lattice parameters (c and a) were calculated using XRD patterns and the CELREF software.

The functional groups of samples were analyzed with Fourier transform infrared (FTIR, Bomem, MB100) in a mid-IR spectrum range in the range of 400–4000 cm^{-1}. For this purpose each powder was mixed with KBr. Mg contents were determined using an atomic absorption spectrophotometer (AAS) (3030). The morphology and agglomerates size distributions of the prepared powders were investigated by scanning electron microscopy, SEM. The morphology and particle size of the powders were checked using Transmission Electron Microscopy (TEM) working at 200 kV.

2.3. In vitro bioactivity evaluation

The SBF was prepared according to the procedure described by Kokubo [18]. The ion concentrations of the SBF are similar to those in human blood plasma. The obtained powders were soaked in the SBF solution (pH 7.4) at 37 °C for 1, 3, 7 and 14 days at a solid/liquid ratio of 1 mg/ml without refreshing the soaking medium.

After soaking for the predicted time periods, the powders were filtered, rinsed with doubly distilled water, and dried in an oven at 80 °C for 24 h before analysis by FTIR and SEM. Ca and Mg concentrations in the SBF solutions were determined by atomic absorption spectrophotometer (AAS, 3030). Phosphate concentrations were determined by spectrophotometer.

3. Results and discussion

Fig. 1a shows the XRD patterns of Mg–FA powders which were sintered at 600 °C. FA diffraction peaks were observed for all samples according to the standard card of FA (JCDP#15-0876). It was found that the position of FA peaks shifted slightly to higher angles with increasing the Mg content of FA powders as shown in Fig. 1b. This suggests that the lattice parameters of FA reduce as a result of the substitution of Ca^{2+} with Mg ions in the FA lattice. On the other hand, since Mg ionic radius (0.065 nm) is smaller than that of Ca^{2+} ions (0.099 nm) [19], the substitution of calcium by smaller Mg ions resulted in a contraction of the cell parameters of FA [19]. The lattice parameters of the obtained powders are listed in Table 1. There

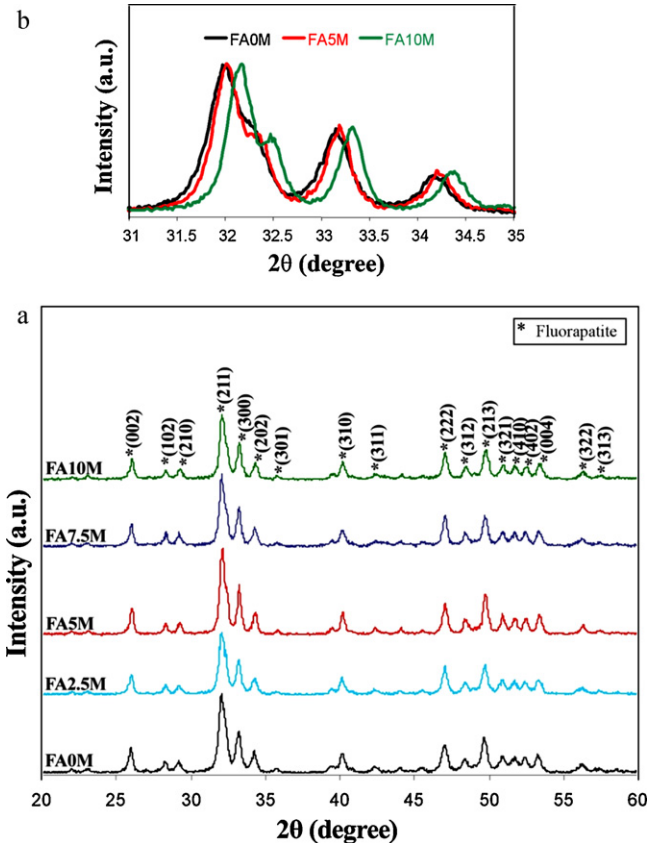

Fig. 1. XRD patterns of Mg–FA nanopowders calcined at 600 °C.

Table 1
Lattice parameters and crystallite size of the obtained nanopowders.

Sample	*a*-Axis (nm)	*c*-Axis (nm)	Crystallite size (nm)
FA0.0M	0.93539	0.68713	46
FA2.5M	0.93491	0.68656	35
FA5.0M	0.93487	0.68650	69
FA7.5M	0.93454	0.68641	35
FA10M	0.93046	0.68433	35

is a large decrease of the unit cell parameters for FA10M in compare to the other samples. Calcium ions in the apatite structure occur in two different locations, Ca(1) and Ca(2). In a real substituted apatite the locations of substituting ions are not necessarily systematic. In neighboring unit cells the ions might be located in different positions [20]. It is suggested that with increasing of Mg content from FA7.5 to FA10M, the Mg ions were substituted in the different position in the FA lattice in compare to the other samples.

The crystallite sizes of the prepared FA with different degrees of Mg content calculated by using XRD data are shown in Table 1. The crystallite size of the obtained nanopowders is in the range of 35–69 nm. Determining crystallite sizes from XRD peak widths makes assumptions on crystallite shape and crystallite size.

Fig. 2 shows the microstructure and morphology of FA5 M powder. The morphology of the powders indicates that it is composed of agglomerates with wide particle size distributions. As shown in Fig. 2c, the agglomerated particles in Fig. 6a and b are composed of very fine particles.

The TEM images of FA5M and FA10M powders (Fig. 3) reveal that the powders are formed by agglomerates of irregular particles ranging from 30 to 100 nm, consistent with values calculated from XRD data.

Chemical analysis of the obtained Mg–FA nanopowders are shown in Fig. 4, where x and x_m are designated and measured Mg concentration, respectively. As can be seen, with increasing x, Mg concentration was increased. In addition, x_m was smaller than x, suggesting that the Mg was partially incorporated into the FA lattice [7]. In other words, Mg in the starting solution partially entered into the FA lattice. Similar results were obtained for hydroxyapatite (HA) [8,19,21,22], which show partial substitution of Ca with Mg in the HA lattice.

Fig. 5 correlates the concentration changes of PO_4^{3-} ions in SBF with the magnesium content in powders for different immersion times. As can be seen, with increasing Mg-substitution, the concentration of PO_4^{3-} ions in SBF was increased, indicating that the solubility increases with the increase in Mg-substitution of FA. The varying solubility trend of Mg–FA obtained in this work is in agreement with previous results that the solubility of apatites increases with increasing ionic substitutions into the apatite lattice [11,23,24].

Fig. 6 correlates the concentration changes of Mg^{2+} in SBF with the magnesium content in powders, for different immersion times. It can be noted that the Mg concentration in the SBF increased with increasing Mg-substitution of powders.

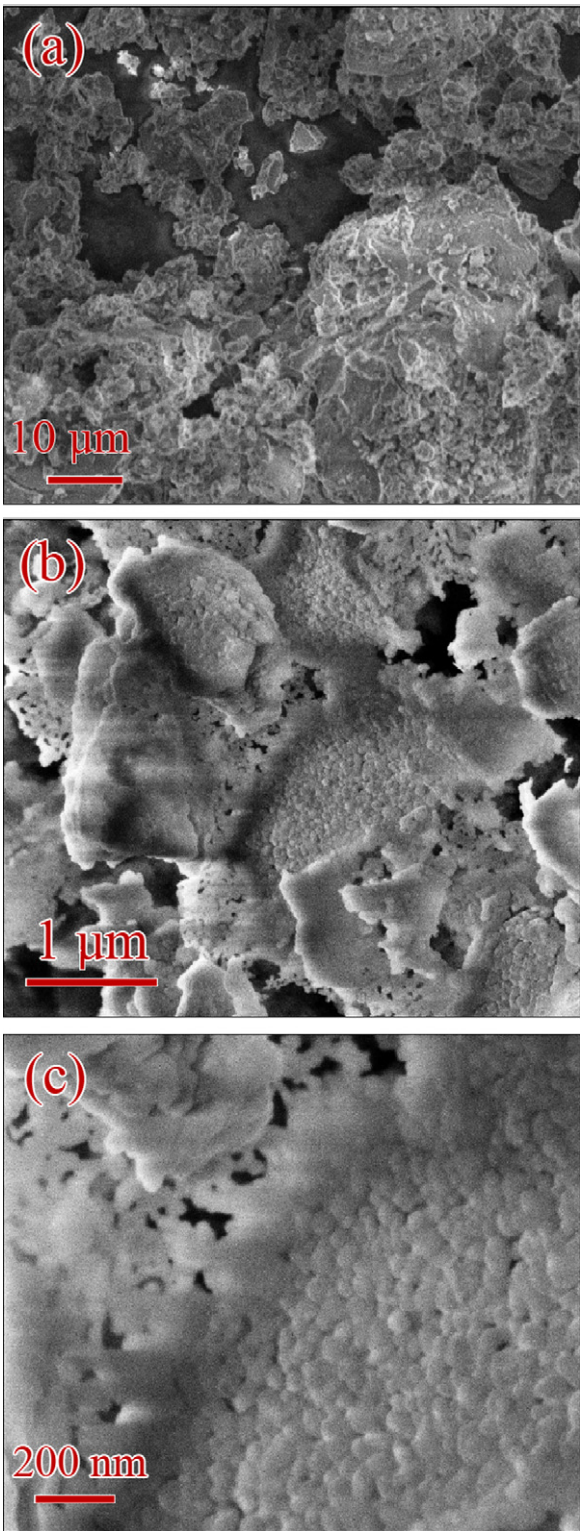

Fig. 2. SEM micrographs of FA5M powder in different magnifications.

The concentration changes of Ca^{2+} ions of the SBF solution after soaking for different immersion times are shown in Fig. 7. As can be seen, with increasing Mg-substitution up to 5%

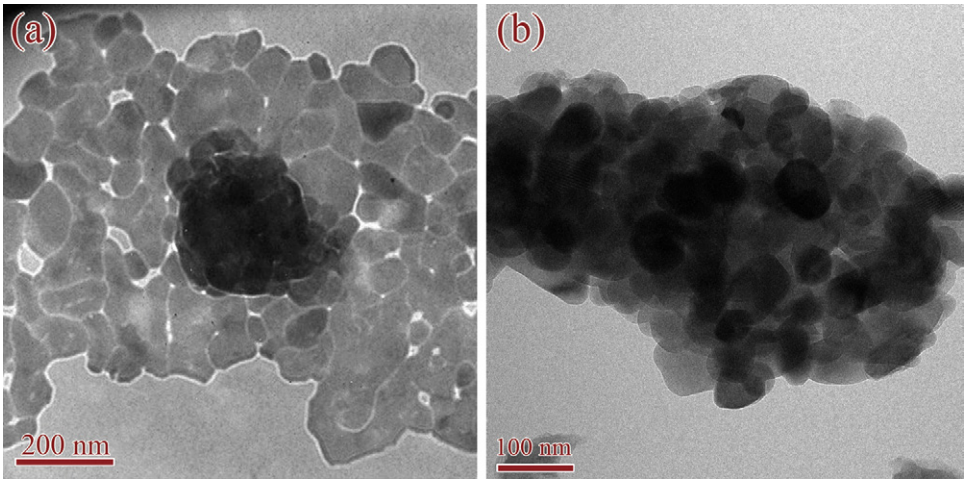

Fig. 3. TEM micrographs of (a) FA5M and (b) FA10M nanopowders calcined at 600 °C.

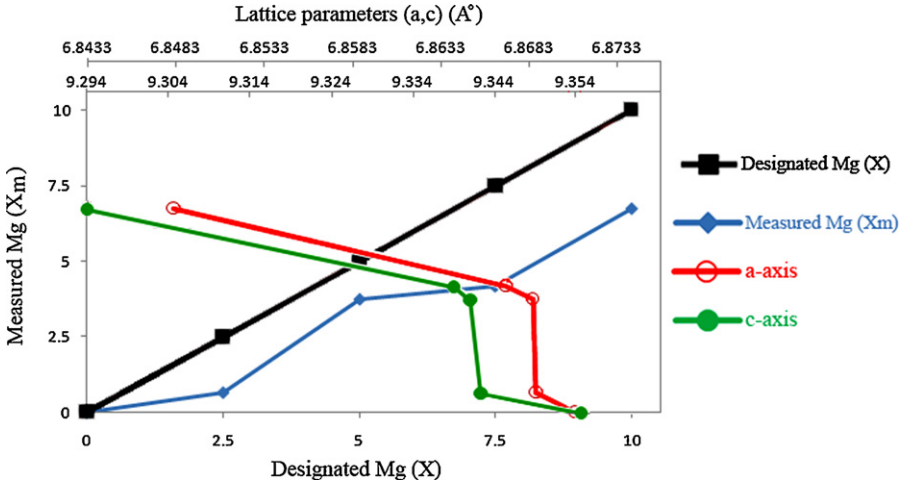

Fig. 4. Changes in measured Mg concentration (X_m) versus different designated Mg (X).

(FA5M), the concentration of Ca^{2+} ions in the SBF was decreased compared to that of pure FA. In contrast, the concentration of Ca^{2+} ions in the SBF for the powders with Mg-substitution more than 5% (FA7.5M and FA10M) was increased compared to that of pure FA.

These behaviors indicate that with increasing the Mg-substitution, the solubility of powders and the precipitation of apatite onto the powders surfaces increased simultaneously. In fact, the Ca^{2+} ions concentration is controlled by

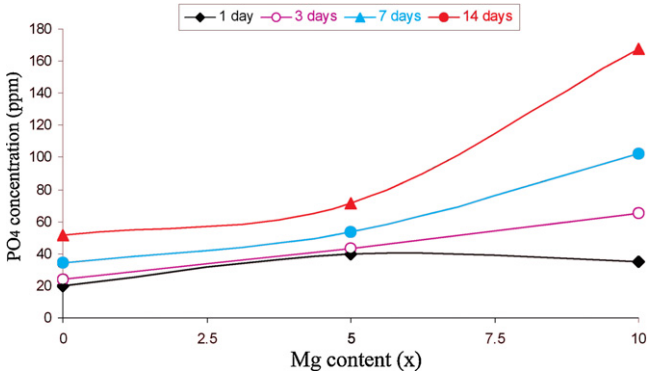

Fig. 5. Concentration changes of PO_4^{3-} ions in SBF after immersion of FA powders with different Mg contents for different immersion times.

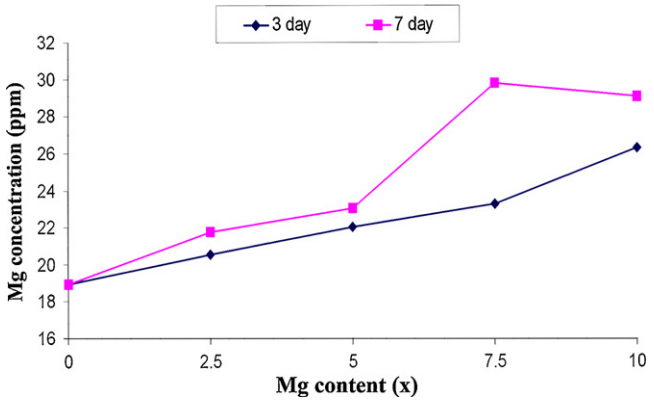

Fig. 6. Concentration changes of Mg^{2+} ions in SBF after immersion of FA powders with different Mg contents for different immersion times.

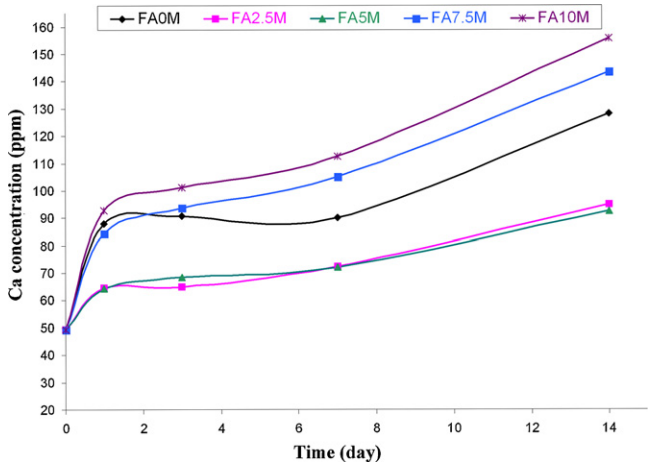

Fig. 7. Concentration changes of Ca^{2+} ions in SBF after immersion of FA powders with different Mg contents for different immersion times.

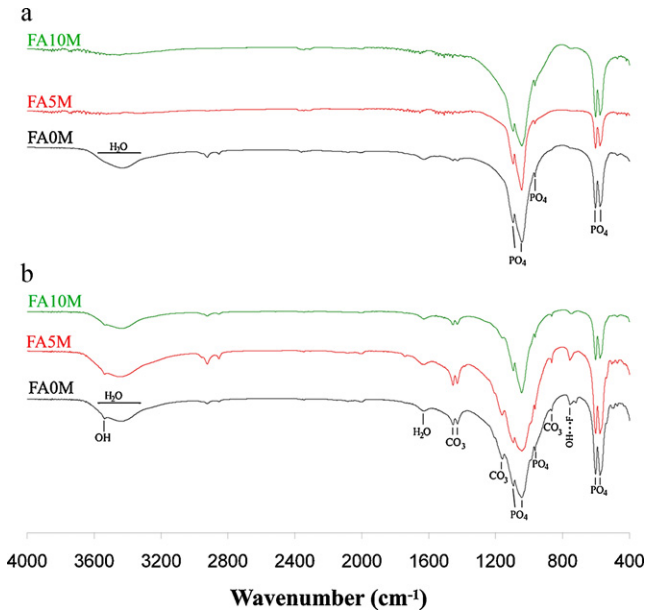

Fig. 8. FTIR spectra of sintered FA powder with different Mg contents: (a) before immersion in SBF; (b) after immersion in SBF 28 days.

both the release of Ca^{2+} ions from the powders and the formation of apatite [25]. When samples are immersed in SBF, both the dissolution of the powders and the precipitation of the new apatite occur at the same time [9]. The decrease in the Ca^{2+} ions concentration in SBF of FA2.5M and FA5M in comparison with that of pure FA is attributed to the favour of precipitation of apatite onto the surface of the powders that overcame the release rate of Ca^{2+} ions to the solution. For FA7.5M and FA10M, the release rate of Ca^{2+} ions to the solution overcame the precipitation of apatite onto the surface of the powders and resulted in increase in the Ca^{2+} concentration in SBF compared to that of pure FA. The differences between the concentration changes of PO_4^{3-} and Ca^{2+} ions resulted from the formation of bone-like apatite (Ca_{10} $(PO4)_{6-x}(CO3)_x(OH)_2$) in which a part of $PO4^{3-}$ was substituted by CO_3^{2-}. This finding is in agreement with other research [16]. The FTIR observation (Fig. 8) confirmed this interpretation. The FTIR spectra of the powders showed the change of the groups of the powders before and after immersion. The bands at 966 and at 474 cm^{-1} were attributed to υ_1 and υ_2 vibration peaks, respectively [19,26]. The absorption peaks located at 1096 and 1045 cm^{-1} were derived from the asymmetrical stretching (υ_3) of PO_4^{3-} and at 577 and 603 cm^{-1} were assigned to the bending modes (υ_4) of PO_4^{3-}, respectively [19]. The bands located at 1632 and 3436 cm^{-1} in IR spectra of FA0M powder were attributed to the water present in the samples and/or absorbed in the KBr pellet [7]. The IR spectra of each of the prepared powders are characteristic of FA [6,7]. After immersion in SBF for 28 days, as Fig. 8 shows, CO_3^{2-} peaks at 865, 1134 [27,28], 1429, and 1455 cm^{-1} and OH^- stretching vibration at 3539 cm^{-1} emerged, confirming the change in the composition of the powders and the formation of bone-like apatite. The band at 758 cm^{-1} were assigned to the OH···F group [6].

The dissolution and precipitation behavior of apatites are the main factors governing their bioactivity [16]. The higher the Mg content in the powders, the faster the dissolution will be. This result is in agreement with previous works related to Mg-substituted hydroxyapatite [9,11]. Therefore, the increase in concentrations of Ca^{2+} and PO_4^{3-} ions resulted in the increase of local supersaturation, which is beneficial to nucleation and growth of the new apatite crystals. In addition, the more the samples dissolved, the more the nucleation sites created. The higher precipitation rate would be obtained in the samples of higher dissolution [16]. Furthermore, it should be noted that Mg is a key-factor for Ca–P coating formation from SBF, and it stimulates deposition of apatite layer directly from SBF [12,29]. Fig. 9 shows SEM micrographs of Mg–FA powders after soaking in the SBF solutions for various time periods. These micrographs show the formation and growth of apatite crystals on the surfaces of the powders after soaking in the SBF solutions for various time periods. As shown in Fig. 9, the higher the Mg-substitution, the faster the apatite crystals grow which confirm the above interpretations.

It is concluded from the analysis of the Ca, Mg and P concentration changes combined with the FTIR result that the bioactivity of the Mg–FA powders is dependent on the Mg concentration of powders because the rate of HA formation determines the bioactivity of the powders [11]. In other words, Mg-substitution improves the bioactivity of FA.

Despite the limitations of the SBF study, examination of apatite formation on the surface of a material in SBF is useful for predicting the in vivo bone bioactivity of the material, not only qualitatively but also quantitatively. This method can be used for screening bone bioactive materials before animal testing and the number of animals used and the duration of animal experiments can be remarkably reduced by using this method [18].

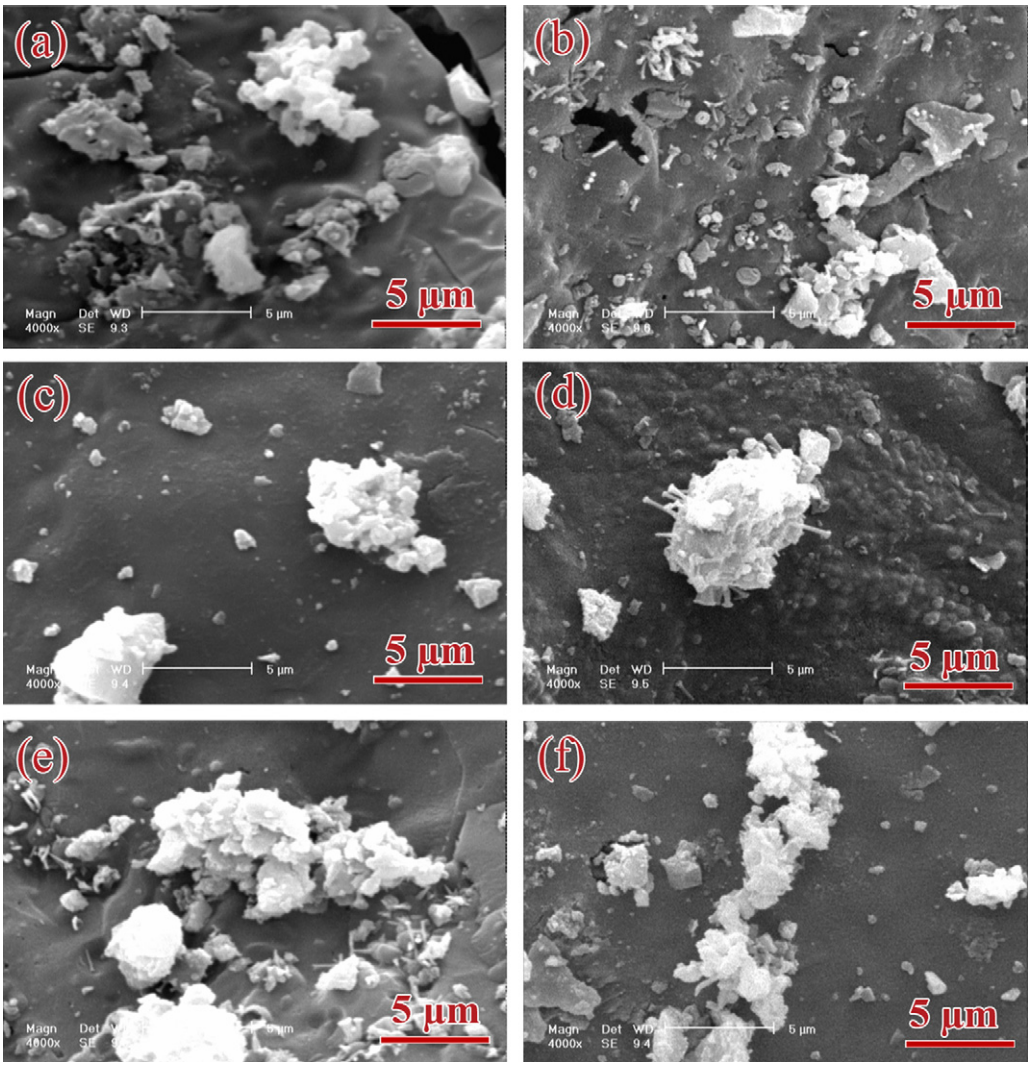

Fig. 9. SEM images of FA0M after soaking in SBF for 3 days(a) and 7 days(b), SEM images of FA5M after soaking in SBF for 3 days(c) and 7 days(d), SEM images of FA10M after soaking in SBF for 3 days(e) and 7 days(f).

4. Conclusions

Mg–FA nanopowders with different Mg contents were prepared by sol–gel method. The in vitro bioactivity of nanopowders was investigated by soaking the powders in SBF. Results indicated that, during synthesis, Mg ions entered into the fluorapatite lattice and occupied Ca^{2+} sites. The obtained nanopowders had crystallite size about 30–100 nm. With increasing the Mg-substitution, the solubility of nanopowders and the adsorption of Ca^{2+} ions onto the powders surfaces increased simultaneously. It was concluded that Mg-substitution improves the bioactivity of FA.

Acknowledgement

The authors are grateful to Isfahan University of Technology for supporting the present research.

References

[1] H. Aoki, Medical Applications of Hydroxyapatite, Ishiyaku Euro America Inc./Takayama Press, Tokyo/St. Louis, 1994.
[2] L.L. Hench, Bioceramics, J. Am. Ceram. Soc. 81 (1998) 1705–1728.
[3] P. Ducheyne, Q. Qiu, Bioactive ceramics: the effect of surface reactivity on bone formation and bone cell function, Biomaterials 20 (1999) 2287.
[4] K. Cheng, G. Shen, W. Weng, G. Han, J.M.F. Ferreira, J. Yang, Synthesis of hydroxyapatite/fluoroapatite solid solution by a sol–gel method, Mater. Lett. 51 (2001) 37–41.
[5] F. Ben Ayed, J. Bouaziz, K. Bouzouita, Calcination and sintering of fluorapatite under argon atmosphere, J. Alloys Compd. 322 (2001) 238–245.
[6] L.M. Rodriguez-Lorenzo, J.N. Hart, K.A. Gross, Influence of fluorine in the synthesis of apatites. Synthesis of solid solutions of hydroxy-fluorapatite, Biomaterials 24 (2003) 3777–3785.
[7] M. Hidouri, K. Bouzouita, F. Kooli, I. Khattech, Thermal behaviour of magnesium-containing fluorapatite, Mater. Chem. Phys. 80 (2003) 496–505.
[8] T.J. Webster, E.A. Massa-Schlueter, J.L. Smith, E.B. Slamovich, Osteoblast response to hydroxyapatite doped with divalent and trivalent cations, Biomaterials 25 (2004) 2111–2121.
[9] W.L. Suchanek, K. Byrappa, P. Shuk, R.E. Riman, V.F. Janas, .K.S. TenHuisen, Mechanochemical–hydrothermal synthesis of calcium phosphate powders with coupled magnesium and carbonate substitution, J. Solid State Chem. 177 (2004) 793–799.
[10] R.Z. LeGeros, Calcium Phosphates in Oral Biology and Medicine, Karger AG, Basel, 1991.

[11] Y. Cai, S. Zhang, X. Zeng, Y. Wang, M. Qian, W. Weng, Improvement of bioactivity with magnesium and fluorine ions incorporated hydroxyapatite coatings via sol–gel deposition on Ti6Al4V alloys, Thin Solid Films 517 (2009) 5347–5351.
[12] H. Liang, Y.Z. Wan, F. He, Y. Huang, J.D. Xu, J.M. Li, Y.L. Wang, Z.G. Zhao, Bioactivity of Mg-ion-implanted zirconia and titanium, Appl. Surf. Sci. 253 (2007) 3326–3333.
[13] C.C. Liu, J.K. Yeh, J.F. Aloia, Magnesium directly stimulates osteoblast proliferation, J. Bone Miner. Res. 3 (1988) S104.
[14] E.A.A. Neel, T. Mizoguchi, M. Ito, M. Bitar, V. Salih, J.C. Knowles, In vitro bioactivity and gene expression by cells cultured on titanium dioxide doped phosphate-based glasses, Biomaterials 28 (2007) 2967–2977.
[15] A.B.Y. Hazar, Preparation and in vitro bioactivity of $CaSiO_3$ powders, Ceram. Int. 33 (2007) 687–692.
[16] Q. Zhang, J. Chen, J. Feng, Y. Cao, C. Deng, X. Zhang, Dissolution and mineralization behaviors of HA coatings, Biomaterials 24 (2003) 4741–4748.
[17] G.K. Williamson, W.H. Hall, X-ray line broadening from filed aluminium and wolfram, Acta Metall. 1 (1953) 22–31.
[18] T. Kokubo, H. Takadama, How useful is SBF in predicting in vivo bone bioactivity, Biomaterials 27 (2006) 2907–2915.
[19] Z. Yang, Y. Jiang, L.X. Yu, B. Wen, F. Li, S. Sun, T. Hou, Preparation and characterization of magnesium doped hydroxyapatite–gelatin nanocomposite, J. Mater. Chem. 15 (2005) 1807–1811.
[20] T. Tamm, M. Peld, Computational study of cation substitutions in apatites, J. Solid State Chem. 179 (2006) 1581–1587.
[21] M. Okazaki, J. Takahashi, H. Kimura, Unstable behavior of magnesium-containing hydroxyapatites, Caries Res. 20 (1986) 324–331.
[22] S.R. Kim, J.H. Lee, Y.T. Kim, D.H. Riu, S.J. Jung, Y.J. Lee, S.C. Chung, Y.H. Kim, Synthesis of Si, Mg substituted hydroxyapatites and their sintering behaviors, Biomaterials 24 (2003) 1389–1398.
[23] W.L. Suchanek, K. Byrappa, P. Shuk, R.E. Riman, V.F. Janas, K.S. TenHuisen, Preparation of magnesium-substituted hydroxyapatite powders by the mechanochemical–hydrothermal method, Biomaterials 25 (2004) 4647–4657.
[24] M.T. Fulmer, I.C. Ison, C.R. Hankermayer, B.R. Constantz, J. Ross, Measurements of the solubilities and dissolution rates of several hydroxyapatites, Biomaterials 23 (2002) 751–755.
[25] A. Saboori, M. Rabiee, F. Moztarzadeh, M. Sheikhi, M. Tahriri, M. Karimi, Synthesis, characterization and in vitro bioactivity of sol–gel-derived SiO_2–CaO–P_2O_5–MgO bioglass, Mater. Sci. Eng. C 29 (2009) 335–340.
[26] Y. Liu, W. Wang, Y. Zhan, C. Zheng, G. Wang, A simple route to hydroxyapatite nanofibers, Mater. Lett. 56 (2002) 496–501.
[27] Y. Liu, L. Luo, G. Chen, M. Xie, Z. Yu, Adsorption of lead ions on ground tyre rubber grafted with maleic anhydride via surface-initiated ATRP polymerization, Iran. Polym. J. 19 (3) (2010) 207–218.
[28] S. Coiai, E. Passaglia, F. Ciardelli, Gradient density grafted polymers on ground tire rubber particles by atom transfer radical polymerization, Macromol. Chem. Phys. 207 (2006) 2289–2298.
[29] F. Barrere, C.A. van Blitterswijk, K. de Groot, P. Layrolle, Nucleation of biomimetic Ca–P coatings on Ti6Al4 V from a SBF × 5 solution: influence of magnesium, Biomaterials 23 (2002) 2211–2220.